Joint Energy and Information Beamforming Design for RIS-assisted Wireless Powered Communication

Zhen Chen, *Member, IEEE*, Jie Tang, *Senior Member, IEEE*, Xiaoyu Du,

Xiuyin Zhang, *Fellow, IEEE*, Daniel Ka Chun So, *Senior Member, IEEE*

and Kai-Kit Wong, *Fellow, IEEE*

Abstract

In the wireless powered communication network (WPCN), the wireless energy acquisition is weak due to the fading characteristic of the wireless link, which is hard to supply energy to wireless sensor. Reconfigurable intelligent surface (RIS) is a promising performance enhancing technology for WPCN, which can improve the energy and spectral efficiency, expand the network coverage, and thus improve the throughput. This paper proposes a new framework for energy harvesting and information transmission of non-orthogonal multiple access (NOMA) based WPCN aided by the RIS. The total transmission capacity is maximized by joint optimization energy beamforming, information beamforming and the RIS phase shift, which turns out to be a non-convex problem. By exploiting the iterative optimization and maximal ratio combining (MRC) algorithm, the energy beamforming and information beamforming are determined for single- and multi-user system, respectively. Numerical results prove that compared with the non-RIS-aided system, the proposed scheme can increase the throughput of the multi-user system.

Index Terms

Reconfigurable intelligent surface (RIS); wireless powered communication network (WPCN); non-orthogonal multiple access (NOMA).

I. INTRODUCTION

The emerging wireless power transfer technology promotes wireless powered networks (WPNs) where nodes are powered by energy access point to communicate with data access point [1]. In order to maintain continuous and uninterrupted information acquisition and transmission, reduce maintenance costs and improve energy efficiency, naturally it has become necessary to supply energy to WSN with environmental energy [2], [3]. Alternatively, the recent advance of radio frequency (RF) enabled wireless power transfer (WPT) provides an attractive solution to power wireless devices over the air. In addition to energy supply through ambient RF signals, an dedicated energy station can be proactively deployed to realize wireless energy transfer (WET) to supply the sensors, which breaks the restriction of passive collection of other

environmental energy, with good controllability [4]. The wireless transmission of information accounts for most of the energy consumption of low-power sensor nodes. From the perspective of improving energy efficiency of information transmission for the wireless sensor nodes, wireless powered communication network (WPCN) has become a research hotspot in the academic community [5]. However, some key challenges still need to be addressed for the deployment of large-scale Internet of Things (IoT), since a large number of WSNs need to be deployed and maintained in various scenarios [6].

Despite the technical advances made, it is still hard even impossible to maintain continuous information transmission for the sensor nodes of a WPCN due to the fading characteristic of wireless links. Reconfigurable intelligent surface (RIS) technology can realize intelligent customization of wireless communication environment, which opens up a new way to effectively improve the quality of wireless link [7]–[10]. RIS can program the signal propagation of the wireless channel by intelligently controlling a large number of passive reflecting elements. RIS-aided wireless communication has received extensive research attention as it can reflect the incident signal with an adjustable phase shift, thereby modifying the radio waves, thus potentially presenting a new milestone in WPCN [11]. Introducing RIS into WPCNs is a relatively new research direction. The introduction of RIS can give full play to the advantages of RIS and improve the throughput performance of WPCNs [12]. In addition, using non-orthogonal multiple access (NOMA) instead of traditional time division multiple access (TDMA) in WPCNs can further improve the throughput of the network [13].

To the best of our knowledge, no research work has yet investigated the design and optimization of energy and information beamforming in RIS-aided WPCN framework. Therefore, it is meaningful to study the impact of jointly energy and information beamforming for RIS-assisted WPCN systems. Specifically, we consider the problem of maximizing the achievable rate, where WET technology and NOMA technology are used to improve the performance of energy harvesting and information transmission. To solve the non-convex optimization problem, a jointly iterative optimization and maximal ratio combining (MRC) algorithm is developed to obtain the maximum channel capacity. Moreover, the energy efficiency of the proposed method outperforms the conventional it is found that exploiting more user diversity is not always beneficial from the perspective of energy efficiency.

II. SYSTEM MODEL AND PROBLEM FORMULATION

A. System model

We consider a multi-user NOMA-based downlink WPCN, which RIS is used to assist the power station (PS) for serving multiple users, as shown in Fig.1. The whole system consists of one power station (PS) with $N_e > 1$ uniform planar array (UPA) transmitting antennas, one access point (AP) with $N_i > 1$ UPA antennas, K information users (IUs) with one antenna and one RIS with M UPA reflecting units, denoted
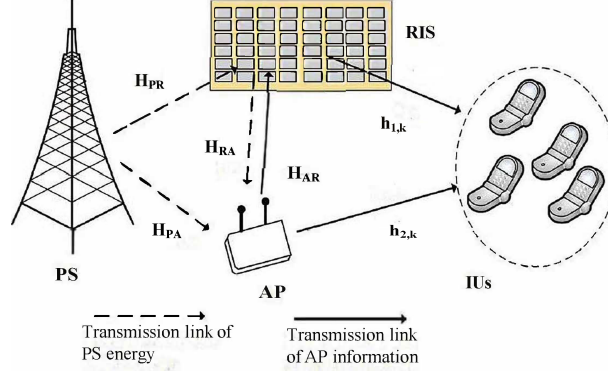
Fig. 1. A multi-user NOMA model based WPCN aided by RIS.

by $\mathcal{K} = \{1, 2, \cdots, K\}$ and $\mathcal{M} = \{1, 2, \cdots, M\}$, respectively. Since the system we designed is a three-dimensional (3D) MIMO system, it is more reasonable to use UPA with one more spatial degree of freedom than uniform linear array (ULA) to model the antenna here. Let $\mathbf{H}_{PR} \in \mathbb{C}^{M \times N_e}, \mathbf{H}_{PA} \in \mathbb{C}^{N_i \times N_e}, \mathbf{H}_{RA} \in \mathbb{C}^{N_i \times M}$, and $\mathbf{H}_{AR} \in \mathbb{C}^{M \times N_i}$ represent baseband equivalent channels from PS to RIS, PS to AP, RIS to AP and AP to RIS, respectively. Meanwhile, $\mathbf{h}_{1,k} \in \mathbb{C}^{M \times 1}$, and $\mathbf{h}_{2,k} \in \mathbb{C}^{N_i \times 1}$ represent the baseband equivalent channels from RIS to IUs and AP to IUs, respectively, $\forall k \in \mathcal{K}$. In addition, we assume the channel state information (CSI) of all channels can be perfectly known.

Next, we model the above channels. For a $P \times Q$ UPA antenna array, its array response can be expressed as

$$\mathbf{a}(\psi, \gamma) = \mathbf{a_x}(\psi, \gamma) \otimes \mathbf{a_y}(\gamma) \tag{1}$$

$$\mathbf{a_x}(\psi, \gamma) = \frac{1}{\sqrt{Q}} \left(\left[1, e^{j\pi(\sin\psi \sin\gamma)}, \ldots, e^{j\pi(P-1)\sin\psi \sin\gamma} \right] \right)^T \tag{2}$$

$$\mathbf{a_y}(\gamma) = \frac{1}{\sqrt{P}} \left(\left[1, e^{j\pi(\cos\gamma)}, \ldots, e^{j\pi(Q-1)\cos\gamma} \right] \right)^T \tag{3}$$

where ψ and γ represent the horizontal angle and the elevation angle, respectively.

For all of above channels, we use the SalehValenzuela channel model that channel $\mathbf{H}_{PR}$ can be expressed as:

$$\mathbf{H}_{PR} = \sum_{l=0}^{L} \frac{\sqrt{N_e M}}{L} \alpha_l \mathbf{a}_{M,l} \left(\psi_M^{(l)}, \gamma_M^{(l)} \right) \mathbf{a}_{N_e,l}^{H} \left(\psi_{N_e}^{(l)}, \gamma_{N_e}^{(l)} \right) \tag{4a}$$

$$\alpha_l = \alpha_0 \left(\frac{d_l}{d_0} \right)^{-\theta} \tag{4b}$$

where $l = 0$ and $l > 0$ represents the line of sight (LoS) and non line of sight (NLoS) path, α_l is plural channel gain for path l, α_0 is path fading at the reference distance d_0, d_l is the link distance, and θ is the path loss exponent. $\psi_{N_e}^{(l)}$ and $\gamma_{N_e}^{(l)}$ represent the horizontal angle and the elevation angle of the l path signal

emitted by PS, and they represent the angle of departure (AoD) in $\mathbf{H}_{PR}$. Similarly, $\psi_M^{(l)}$ and $\gamma_M^{(l)}$ correspond to the angle of arrival (AoA) in $\mathbf{H}_{PR}$. Other channels are built by similar methods.

For the energy harvesting link, the energy received at the AP can be expressed as:

$$\mathbf{y}_{AP-PS} = \left(\mathbf{H}_{RA}\mathbf{\Theta}\mathbf{H}_{PR} + \mathbf{H}_{PA}\right)\mathbf{G}\mathbf{s} + \mathbf{n}_1, \tag{5}$$

where $\mathbf{\Theta} = \mathrm{diag}\left(\beta_1 e^{j\theta_1}, \ldots, \beta_M e^{j\theta_M}\right) \in \mathbb{C}^{M \times M}$ denotes the reflection coefficients matrix of RIS. β_m and θ_m denote the amplitude reflection coefficient and phase shift of the m-th reflecting element. Consider the reflecting element of the RIS is designed to maximize the reflected signal, thus $\beta_m = 1, \forall m \in \mathcal{M}$ and only consider adjusting the phase θ_m of the RIS to maximize the reflected signal. $\mathbf{G} \in \mathbb{C}^{N_e \times N_e}$ is the energy beamforming matrix of the PS. $\mathbf{s} \in \mathbb{C}^{N_e \times 1}$ is the transmission data symbol for PS and it is an independent identically distributed circular symmetric complex Gaussian random signal with zero mean and covariance $\mathbb{E}\left[\mathbf{s}\mathbf{s}^{\mathrm{H}}\right] = \mathbf{I}_{\mathbf{N_t}}$[45]. $\mathbf{n}_1 \sim C\mathcal{N}(0, \delta^2)$ is the noise received at the AP.

In the information transmission link, the baseband transmitted signal of the AP can be expressed as:

$$\mathbf{x} = \sum_{k=1}^{K} \mathbf{w}_k x_k, \forall k \in \mathcal{K}, \tag{6}$$

where $\mathbf{w}_k \in \mathbb{C}^{N_i \times 1}$ is the information beamforming vector for the k-th IUs, $x_k \sim C\mathcal{N}(0, 1), k \in \mathcal{K}$ denotes the transmission data symbol for the k-th IU. $\mathbf{x}$ means that the beamforming information of K users is sent at the same time. So the information received at the k-th IU is:

$$\mathbf{y}_{IU,k-AP} = \left(\mathbf{h}_{1,k}^{\mathrm{H}}\mathbf{\Theta}\mathbf{H}_{AR} + \mathbf{h}_{2,k}^{\mathrm{H}}\right) \sum_{j=1}^{K} \mathbf{w}_j x_j + n_{2,k}, \forall k \in \mathcal{K} \tag{7}$$

where $n_{2,k} \sim C\mathcal{N}(0, \delta^2)$ is the noise received at the k-th IU.

In this system, we only consider downlink information transmission. In conventional NOMA communication, when we use successive interference cancellation (SIC) demodulation technology at the IUs, the signal-interference-plus-noise ratio (SINR) at the k-th IU can be expressed as:

$$\Gamma_k(\mathbf{w}, \mathbf{G}, \mathbf{\Theta}) = \frac{\left|\left(\mathbf{h}_{1,k}^{\mathrm{H}}\mathbf{\Theta}\mathbf{H}_{AR} + \mathbf{h}_{2,k}^{\mathrm{H}}\right)\mathbf{w}_k\right|^2}{\sum_{x(j)>x(k)}\left|\left(\mathbf{h}_{1,k}^{\mathrm{H}}\mathbf{\Theta}\mathbf{H}_{AR} + \mathbf{h}_{2,k}^{\mathrm{H}}\right)\mathbf{w}_j\right|^2 + \delta^2} \tag{8}$$

where $\forall k \in \mathcal{K}$, and $\mathbf{w} \in \mathbb{C}^{N_i \times 1}$ represents the information beamforming vector of every IUs. $\left|\left(\mathbf{h}_{1,k}^{\mathrm{H}}\mathbf{\Theta}\mathbf{H}_{AR} + \mathbf{h}_{2,k}^{\mathrm{H}}\right)\mathbf{w}_k\right|^2$ is the received signal power in k-th IU and $\sum_{x(j)>x(k)}\left|\left(\mathbf{h}_{1,k}^{\mathrm{H}}\mathbf{\Theta}\mathbf{H}_{AR} + \mathbf{h}_{2,k}^{\mathrm{H}}\right)\mathbf{w}_j\right|^2$ is the interference power from other IUs. The SIC decoding order $x(k)$ is depending by channal conditions from AP to the IUs. The better the channel conditions, the later the decoding order. $x(k) = i$ denotes that the k-th IU is the i-th signal to be decoded at the receiver. So when $x(j) > x(k)$, it means that $x(j)$ demodulated after $x(k)$, that is, it will cause interference to the k-th user. In other words, IUs will only be interfered by IUs with better communication channel condition. δ^2 is noise power.

B. Problem formulation

In order to obtain the maximum channel capacity of the multi-user NOMA model based WPCN aided by RIS, it is considered that the reflection coefficients matrix Θ of the RIS, the energy beamforming $\mathbf{G}$ of the PS and the information beamforming $\mathbf{w}$ of AP should be jointly optimized. According to Shannon formula, the optimization function can be expressed as:

$$\max: R(\mathbf{w}, \mathbf{G}, \Theta) = \sum_{k=1}^{K} \log_2\left(1 + \Gamma_k(\mathbf{w}, \mathbf{G}, \Theta)\right), \forall k \in \mathcal{K} \tag{9a}$$

$$\text{s.t. } C1: P_1 = \sum_{j=1}^{K} \|\mathbf{w}_j\|^2 \leqslant \|(\mathbf{H}_{RA}\Theta\mathbf{H}_{PR} + \mathbf{H}_{PA})\,\mathbf{G}\|_F^2, \tag{9b}$$

$$C2: \mathrm{Tr}\left(\mathbf{G}\mathbf{G}^{\mathrm{H}}\right) \leqslant P_0, \tag{9c}$$

$$C3: 0 < \theta_i \leqslant 2\pi \tag{9d}$$

$$C4: \Gamma_k(\mathbf{w}, \mathbf{G}, \Theta) > \gamma_{\min,k}. \tag{9e}$$

where the objective function and $C4$ constraint is a tightly coupled non-convex functions. P_0 in the $C2$ constraint represents the maximum transmit power of PS. There is no way to find the maximum value of the objective function directly.

Then, introduce ς_k and replace $\Gamma_k(\mathbf{w}, \mathbf{G}, \Theta)$ in the objective function so that the objective function is now a convex function:

$$\max: R(\mathbf{w}, \mathbf{G}, \Theta) = \sum_{k=1}^{K} \log_2\left(1 + \varsigma_k\right), \forall k \in \mathcal{K}, \tag{10a}$$

$$\text{s.t. } C1: P1 = \sum_{j=1}^{K} \|\mathbf{w}_j\|^2 \leqslant \|(\mathbf{H}_{RA}\Theta\mathbf{H}_{PR} + \mathbf{H}_{PA})\,\mathbf{G}\|_F^2, \tag{10b}$$

$$C2: \mathrm{Tr}\left(\mathbf{G}\mathbf{G}^{\mathrm{H}}\right) \leqslant P_0, \tag{10c}$$

$$C3: 0 < \theta_i \leqslant 2\pi \tag{10d}$$

$$C4: \varsigma_k > \gamma_{\min,k}, \tag{10e}$$

$$C5: \Gamma_k(\mathbf{w}, \mathbf{G}, \Theta) \geqslant \varsigma_k. \tag{10f}$$

where $\Gamma_k(\mathbf{w}, \mathbf{G}, \Theta)$ is a union non-convex function because of the tight coupling between $\mathbf{w}, \mathbf{G}$, and Θ. It will be simplified and deformed in the next section.

III. THE PROPOSED ASS OPTIMIZATION ALGORITHM FOR RIS-ASSISTED NOMA SYSTEM

In this section, we propose an ASS optimization algorithm to solve the problem in Equation (10) which is tightly coupled. The problem is decoupled into two stages.

A. Pretreatment

For the energy beamforming $\mathbf{G}$ of PS, we adopt the beamforming strategy [14] to maximize the energy received by the AP. Therefore, the energy of PS can be precoded as

$$\mathbf{G} = \mathbf{b}_1 \mathbf{b}_1^{\mathrm{H}}, \tag{11}$$

where $\Gamma_k(\mathbf{w}, \mathbf{G}, \boldsymbol{\Theta})$ is a tightly coupled function only about $\mathbf{w}$ and $\boldsymbol{\Theta}$. Before using the AO algorithm, the optimization function (10) can be further simplified. For the $C5$ constraint, $\boldsymbol{\theta}$ is converted into the form of vector $\mathbf{v} = \left(e^{j\theta_1}, \ldots, e^{j\theta_M} \right)$. So $\Gamma_k(\mathbf{w}, \mathbf{G}, \boldsymbol{\Theta})$ becomes $\Gamma_k(\mathbf{w}, \mathbf{b}_1, \mathbf{v})$.

In addition, the signal received at the k-th IU can be re-expressed as:

$$\left(\mathbf{h}_{1,k}^{\mathrm{H}} \boldsymbol{\Theta} \mathbf{H_{AR}} + \mathbf{h}_{2,k}^{\mathrm{H}} \right) \mathbf{w}_k = \left(\mathbf{v} \mathbf{R}_{1,k} + \mathbf{h}_{2,k}^{\mathrm{H}} \right) \mathbf{w}_k, \tag{12}$$

where $\mathbf{R}_{1,k} = \mathrm{diag}\left(\mathbf{h}_{1,k} \right) \mathbf{H}_{AR}$. This form of formula (12) helps us to further optimize. At the same time, we define $\tilde{\mathbf{v}} = [\mathbf{v}, 1]$, $\tilde{\mathbf{R}}_{1,k} = \left[\mathbf{R}_{1,k}, \mathbf{h}_{2,k}^{\mathrm{H}} \right]^{\mathrm{T}}$. Therefore, $\Gamma_k(\mathbf{w}, \mathbf{b}_1, \mathbf{v})$ could be rewritten as

$$\Gamma_k(\mathbf{w}, \mathbf{b}_1, \tilde{\mathbf{v}}) = \frac{\left| \tilde{\mathbf{v}} \tilde{\mathbf{R}}_{1,k} \mathbf{w}_k \right|^2}{\sum_{x(j) > x(k)} \left| \tilde{\mathbf{v}} \tilde{\mathbf{R}}_{1,k} \mathbf{w}_j \right|^2 + \delta^2}. \tag{13}$$

For the Frobenius norm of $C1$ constraint, it can be expanded into the following Eq.(14). It is assumed that the signal is transmitted at the maximum power P_0 allowed by the PS.

$$\mathbf{R}_0 = \mathbf{H}_{RA} \, \mathrm{diag}\left(\mathbf{H}_{PR} \mathbf{b}_1 \right),$$

$$\mathbf{T}_0 = \begin{bmatrix} \mathbf{R}_0^{\mathrm{H}} \mathbf{R}_0 & \mathbf{R}_0^{\mathrm{H}} \mathbf{H}_{PA} \mathbf{b}_1 \\ \left(\mathbf{H}_{PA} \mathbf{b}_1 \right)^{\mathrm{H}} \mathbf{R}_0 & \left(\mathbf{H}_{PA} \mathbf{b}_1 \right)^{\mathrm{H}} \mathbf{H}_{PA} \mathbf{b}_1 \end{bmatrix}, \tag{14}$$

$$P_1 \leqslant P_0 \tilde{\mathbf{v}} \mathbf{T}_0 \tilde{\mathbf{v}}^{\mathrm{H}}$$

Therefore, the problem (10) can be transformed into:

$$\mathcal{P}_0 : \max R(\mathbf{w}, \tilde{\mathbf{v}}) = \sum_{k=1}^{K} \log_2 \left(1 + \varsigma_k \right), \forall k \in \mathcal{K}, \tag{15a}$$

$$\text{s.t. } C1 : P_1 \leqslant P_0 \tilde{\mathbf{v}} \mathbf{T}_0 \tilde{\mathbf{v}}^{\mathrm{H}}, \tag{15b}$$

$$C3 : 0 < \theta_i \leqslant 2\pi, \tag{15c}$$

$$C4 : \varsigma_k > \gamma_{\min,k}, \tag{15d}$$

$$C5 : \Gamma_k(\mathbf{w}, \mathbf{b}_1, \tilde{\mathbf{v}}) \geqslant \varsigma_k. \tag{15e}$$

where $C5$ is still non-convex and needs further processing. Next, we will use the AO algorithm to solve this optimization function.

B. Optimizing by fixing phase shift matrix Θ

When the phase matrix Θ is fixed, correspondingly $\tilde{\mathbf{v}}$ is also determined. Therefore, $\Gamma_k(\mathbf{w}, \mathbf{b}_1, \tilde{\mathbf{v}})$ can be rewritten as:

$$
\Gamma_k(\mathbf{\Omega}) = \frac{\left| \tilde{\mathbf{v}} \tilde{\mathbf{R}}_{1,k} \mathbf{w}_k \right|^2}{\sum_{x(j)>x(k)} \left| \tilde{\mathbf{n}} \tilde{\mathbf{R}}_{1,k} \mathbf{w}_j \right|^2 + \delta^2},
$$

$$
= \frac{\tilde{\mathbf{v}} \tilde{\mathbf{R}}_{1,k} \mathbf{\Omega}_k \tilde{\mathbf{R}}_{1,k}^{\mathrm{H}} \tilde{\mathbf{r}}^{\mathrm{H}}}{\sum_{x(j)>x(k)} \tilde{\mathbf{v}} \tilde{\mathbf{R}}_{1,k} \mathbf{\Omega}_j \tilde{\mathbf{R}}_{1,k}^{\mathrm{H}} \tilde{\mathbf{v}}^{\mathrm{H}} + \delta^2}, \tag{16}
$$

where $\Omega_k = \mathbf{w}_k \mathbf{w}_k^{\mathrm{H}}$. Based on SDR, the optimization problem can be rewritten as problem $\mathcal{P}_1$, i.e.,

$$
\mathcal{P}_1 : \max R(\mathbf{\Omega}) = \sum_{k=1}^{K} \log_2 (1 + \varsigma_k), \forall k \in \mathcal{K}, \tag{17a}
$$

$$
s.t.C1 : P_1 \leqslant P_0 \tilde{\mathbf{v}} \mathbf{T}_0 \tilde{\mathbf{v}}^{\mathrm{H}}, \tag{17b}
$$

$$
C3 : 0 < \theta_i \leqslant 2\pi, \tag{17c}
$$

$$
C4 : \varsigma_k > \gamma_{\min,k}, \tag{17d}
$$

$$
\bar{C}5 : \frac{\tilde{\mathbf{v}} \tilde{\mathbf{R}}_{1,k} \mathbf{\Omega}_k \tilde{\mathbf{R}}_{1,k}^{\mathrm{H}} \tilde{\mathbf{v}}^{\mathrm{H}}}{\sum_{x(j)>x(k)} \tilde{\mathbf{v}} \tilde{\mathbf{R}}_{1,k} \mathbf{\Omega}_j \tilde{\mathbf{R}}_{1,k}^{\mathrm{H}} \tilde{\mathbf{v}}^{\mathrm{H}} + \delta^2} \geqslant s_k, \tag{17e}
$$

$$
C6 : \mathbf{\Omega}_k \geq 0. \tag{17f}
$$

It is worth mentioning that it is still non-convex, because $\bar{C}5$ is still a non-convex constraint, we can apply SCA to solve it. According to [15], introduce auxiliary variables a_k and b_k which satisfied that:

$$
\tilde{\mathbf{V}} \tilde{\mathbf{R}}_{1,k} \mathbf{\Omega}_k \tilde{\mathbf{R}}_{1,k}^{\mathrm{H}} \tilde{\mathbf{v}}^{\mathrm{H}} \geqslant e^{a_k+b_k} + \delta^2 e^{b_k}, \tag{18}
$$

$$
e^{a_k} \geqslant \sum_{x(j)>x(k)} \tilde{\mathbf{v}} \tilde{\mathbf{R}}_{1,k} \mathbf{\Omega}_j \tilde{\mathbf{R}}_{1,k}^{\mathrm{H}} \tilde{\mathbf{v}}^{\mathrm{H}} \tag{19}
$$

$$
e^{b_k} \geqslant \varsigma_k \tag{20}
$$

The first-order Taylor expansion of a_k and b_k at the feasible point $\left\{ a_k^{(t)}, b_k^{(t)} \right\}$ can be seen as the lower bound. $\mathcal{P}_1$ can be obtained by $\mathcal{P}_2$, which can be solved by the convex optimization method.

$$\mathcal{P}_2 : \max R\left(\mathbf{\Omega}, a_k, b_k\right) = \sum_{k=1}^{K} \log_2\left(1 + s_k\right), \forall k \tag{21a}$$

$$\text{s.t. } C1 : P_1 \leqslant P_0 \tilde{\mathbf{v}}_0 \tilde{\mathbf{v}}^{\mathrm{H}} \tag{21b}$$

$$C3 : 0 < \theta_i \leqslant 2\pi, \tag{21c}$$

$$C4 : \varsigma_k > \gamma_{\min,k}, \tag{21d}$$

$$\bar{C}5.a : \tilde{\mathbf{v}}\tilde{\mathbf{R}}_{1,k}\mathbf{\Omega}_k\tilde{\mathbf{R}}_{1,k}^{\mathrm{H}}\tilde{\mathbf{v}}^{\mathrm{H}} \geqslant e^{a_k+b_k} + \delta^2 e^{b_k} \tag{21e}$$

$$\bar{C}5.b : e^{a_k^{(t)}} + e^{a_k^{(t)}}\left(a_k - a_k^{(t)}\right) \geqslant \sum_{x(j)>x(k)} \tilde{\mathbf{v}}\tilde{\mathbf{R}}_{1,k}\mathbf{\Omega}_j\tilde{\mathbf{R}}_{1,k}^{\mathrm{H}}\tilde{\mathbf{v}}^{\mathrm{H}} \tag{21f}$$

$$\bar{C}5.c : e^{b_k^{(t)}} + e^{b_k^{(t)}}\left(b_k - b_k^{(t)}\right) \geqslant s_k, \tag{21g}$$

$$C6 : \mathbf{\Omega}_k \geq 0. \tag{21h}$$

This is a convex optimization problem and could be solved easily.

C. Optimizing by fixing information beamforming $\mathbf{w}$

Fixing $\mathbf{w}$, the $\Gamma_k\left(\mathbf{w}, \mathbf{b}_1, \tilde{\mathbf{v}}\right)$ can be rewritten as:

$$\begin{aligned} \Gamma_k(\mathbf{V}) &= \frac{\left|\tilde{\mathbf{v}}\tilde{\mathbf{R}}_{1,k}\mathbf{w}_k\right|^2}{\sum_{x(j)>x(k)}\left|\tilde{\mathbf{R}}_{1,k}\mathbf{w}_j\right|^2 + \delta^2}, \\ &= \frac{\mathbf{w}_k^{\mathrm{H}}\tilde{\mathbf{R}}_{1,k}^{\mathrm{H}}\mathbf{V}\tilde{\mathbf{R}}_{1,k}\mathbf{w}_k}{\sum_{x(j)>x(k)}\mathbf{w}_j^{\mathrm{H}}\tilde{\mathbf{R}}_{1,k}^{\mathrm{H}}\mathbf{V}\tilde{\mathbf{R}}_{1,k}\mathbf{w}_j + \delta^2}, \end{aligned} \tag{22}$$

where $\mathbf{V} = \tilde{\mathbf{v}}^{\mathrm{H}}\tilde{\mathbf{v}}$.

Similarly, after introducing SDR and introducing auxiliary variables x_k, y_k, the optimization function can

be expressed as $\mathcal{P}_3$:

$$\mathcal{P}_3 : \max R\left(\mathbf{V}, x_k, y_k\right) = \sum_{k=1}^{K} \log_2\left(1 + \varsigma_k\right), \forall k \in \mathcal{K}, \tag{23a}$$

$$\text{s.t. } C1 : P_1 \leqslant P_0 \tilde{\mathbf{v}} \mathbf{T}_0 \tilde{\mathbf{v}}^{\mathrm{H}}, \tag{23b}$$

$$C3 : 0 < \theta_i \leqslant 2\pi, \tag{23c}$$

$$C4 : \varsigma_k > \gamma_{\min,k}, \tag{23d}$$

$$\bar{C}5.a : \mathbf{w}_k^{\mathrm{H}} \tilde{\mathbf{R}}_{1,k}^{\mathrm{H}} \mathbf{V} \tilde{\mathbf{R}}_{1,k} \mathbf{w}_k \geqslant e^{x_k + y_k} + \delta^2 e^{y_k}, \tag{23e}$$

$$\bar{C}5.b : e^{x_k^{(t)}} + e^{x_k^{(t)}} \left(x_k - x_k^{(t)}\right) \tag{23f}$$

$$\geqslant \sum_{x(j) > x(k)} \mathbf{w}_j^{\mathrm{H}} \tilde{\mathbf{R}}_{1,k}^{\mathrm{H}} \mathbf{V} \tilde{\mathbf{R}}_{1,k} \mathbf{W}_j, \tag{23g}$$

$$\bar{C}5.c : e^{y_k^{(t)}} + e^{y_k^{(t)}} \left(y_k - y_k^{(t)}\right) \geqslant \varsigma_k \tag{23h}$$

$$C6 : \mathbf{V} \succeq 0 \tag{23i}$$

$$C7 : \mathbf{V}_{m,m} = 1, m = 1, 2, \cdots, M + 1 \tag{23j}$$

Obviously, Problem $\mathcal{P}_3$ can be solved by convex optimization method.

Algorithm 1 ASS algorithm

1: **Initialization**: $t = 0, \mathbf{V}^{(t)}, l_{th} \to 0$;

2: **while until** $\mathbf{V}^{(t)} - \mathbf{V}^{(t-1)} > l_{th}$**do**;

3:     Solve the Problem $(\mathcal{P}_2)$ to calculate $\mathbf{\Omega}_k^*$,
        according to $\mathbf{V}^{(t)}, \mathbf{\Omega}_k^{(t)} = \mathbf{\Omega}_k^*$;

4:     Solve the Problem $(\mathcal{P}_3)$ to calculate $\mathbf{V}^*$,
        according to $\mathbf{\Omega}_k^{(t)}, \mathbf{V}^{(t)} = \mathbf{V}^*$;

5:     $t = t + 1$;

6: **end while**

7: **Output:**

8: Use the obtained $\mathbf{V}^*$ and $\mathbf{\Omega}_k^*$ to calculate the optimal
   throughput.

The proposed algorithm process is listed in Algorithmt 1. Specifically, the step 1 is to randomly initialize $\mathbf{V}^{(0)}$ that meets the conditions as the initial input. Step 2 is based on $\mathbf{V}^{(t)}$ and each channel matrix are calculated by solving problem $\mathcal{P}_2$ to get $\mathbf{\Omega}_k^*$, and let normal $\mathbf{\Omega}_k^{(t)} = \mathbf{\Omega}_k^*$ which is used for the next input. The step 3 is according to $\mathbf{\Omega}^{(t)}$ and each channel matrix to calculate the $\mathbf{V}^*$ by solving problem $\mathcal{P}_3$, and
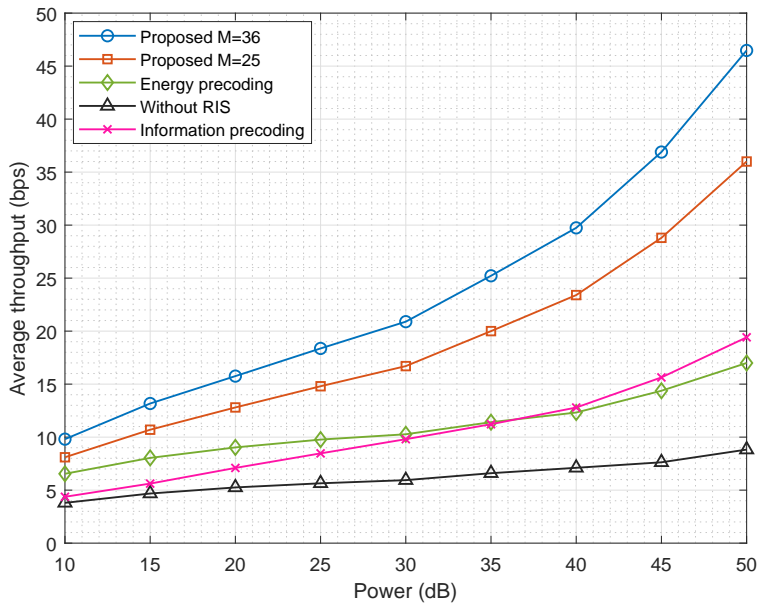
Fig. 2. Average throughput vs transmission power P_0.

$\mathbf{V}^{(t)} = \mathbf{V}^*$. Repeat until the difference between the results of the two cycles is less than the preset threshold. Using the obtained $\mathbf{V}^*$ and $\boldsymbol{\Omega}_k^*$ is used to calculate the optimal throughput.

IV. NUMERICAL RESULTS

Numerical results verify the performance of our proposed ASS algorithm by jointly optimizing energy beamforming, information beamforming, and RIS phase shift matrix scheme for the multi-user system. We consider a three-dimensional (3D) Cartesian coordinate system, where the PS, RIS and AP placed on the buiding are located at $(0\text{ m}, 0\text{ m}, 2\text{ m}), (0\text{ m}, 2\text{ m}, 2\text{ m})$ and $(2\text{ m}, 0\text{ m}, 0\text{ m})$, respectively. And $\mathcal{K} = 4$ IUs randomly distribute at the quarter circle with center $(0\text{ m}, 0\text{ m}, 0\text{ m})$, starting point $(20\text{ m}, 0\text{ m}, 0\text{ m})$ and ending point $(0\text{ m}, 20\text{ m}, 0\text{ m})$ with anti-clockwise. The following parameters will be used in the simulation. The number of PS antennas is $N_e = 4$. The number of AP antennas is $N_i = 4$. The number of reflecting units M in RIS is 9. The noise power is set as -70dBm and the transmission power P_0 of PS are set as 20dBm. The corresponding path loss exponent θ between PS and RIS, PS and AP, and RIS and AP are all 2. While the corresponding path loss exponent θ between the IUs and the AP is 3.5. The convergence thresholds are set to 10^{-3}. We make $\alpha_0 = -30dB, d_0 = 1$.

Fig.2 compare the change of average throughput with the increase of transmission power P_0 in PS when $M = 25$. We can see that the average throughput of each algorithm increases gradually with the increase of transmission power. Compared with other conditions, our proposed ASS algorithm can obtain the best performance at any power. Moreover, with the increase of transmitting power, the distance between ASS algorithm and other conditions will become larger. This is because the ASS algorithm optimizes both
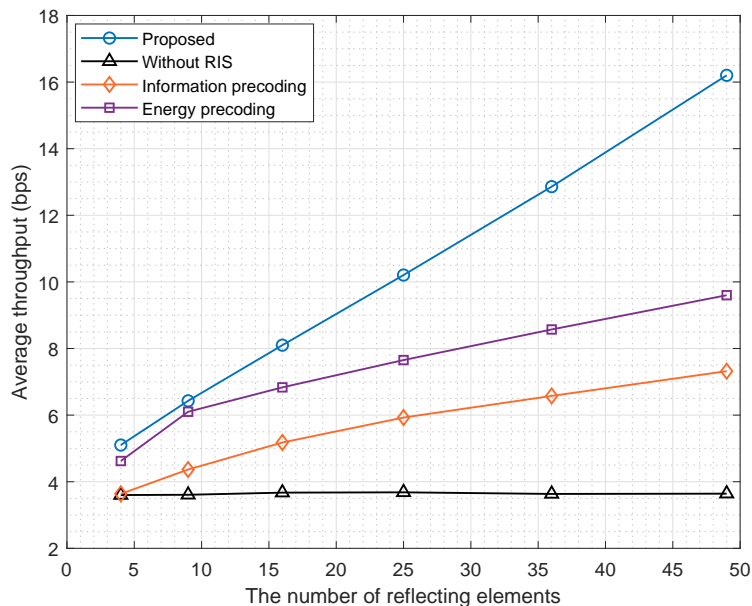
Fig. 3. Average throughput vs reflecting elements number of RIS.

energy beamforming and information beamforming by adjusting the RIS phase shift, and makes a trade-off between them to obtain the maximum system throughput. For the individual energy beamforming and information beamforming, one can only improve the collected energy, and the other can optimize information beamforming, so the maximum throughput can not be obtained naturally. As for the performance without RIS, it is always the worst. In addition, we improved M to 36 for further experiments. We can also observe that the throughput of the system will increase with the increase of the number of RIS reflecting elements.

Then, we compare the effect of the RIS reflecting elements number M on average throughput in Fig.3. It can be seen that the average throughput performance of the proposed ASS algorithm, the information beamforming and the energy beamforming increases when the number of RIS reflecting elements increases. However, the condition without RIS has no effect because there is no RIS. In addition, the performance of proposed algorithm is about two times higher when the number of reflecting elements is only 4 than condition without RIS. RIS components are low cost passive devices, laying a large number of RIS components will not bring too much cost consumption. Therefore, it is worth noting that when the number of reflecting elements is increased to 36, the performance is even five times higher.

V. CONCLUSION

In this paper, we proposed a robust beamforming scheme, which strikes a balance between the beamforming gain and the channel error, and the importance of exploiting both the passive beamforming of RIS and flexible deployment in designing multi-RIS assisted wireless communications. We formulated an WSM

problem that maximizes the beamforming gain and minimizes the channel estimation error at the same time. The closed-form FP method was employed to make the non-convex WSM problem. Furthermore, to alleviate the effects of the channel estimation error and RIS placement, the joint optimization of transmit/reflect beamforming, channel error and RIS placement algorithm was designed to overcome the channel uncertainty and RIS placement. The simulation results demonstrated that the developed approach is effective compared with conventional benchmark schemes.

REFERENCES

[1] C. Han, L. Chen, and W. Wang, "Compressive sensing in wireless powered network: Regarding transmission as measurement," *IEEE Wireless Communications Letters*, vol. 8, no. 6, pp. 1709–1712, 2019.

[2] X. Lu, P. Wang, D. Niyato, D. I. Kim, and Z. Han, "Wireless charging technologies: Fundamentals, standards, and network applications," *IEEE Communications Surveys & Tutorials*, vol. 18, no. 2, pp. 1413–1452, 2016.

[3] Z. Chen, Z. Chen, L. X. Cai, and Y. Cheng, "Optimal beamforming design for simultaneous wireless information and power transfer in sustainable cloud-RAN," *IEEE Transactions on Green Communications and Networking*, vol. 2, no. 1, pp. 163–174, 2018.

[4] T. Ruan, Z. J. Chew, and M. Zhu, "Energy-aware approaches for energy harvesting powered wireless sensor nodes," *IEEE Sensors Journal*, vol. 17, no. 7, pp. 2165–2173, 2017.

[5] Q. Yao, T. Q. S. Quek, A. Huang, and H. Shan, "Joint downlink and uplink energy minimization in WET-enabled networks," *IEEE Transactions on Wireless Communications*, vol. 16, no. 10, pp. 6751–6765, 2017.

[6] M. Zuhair, F. Patel, D. Navapara, P. Bhattacharya, and D. Saraswat, "Blocov6: A blockchain-based 6g-assisted uav contact tracing scheme for covid-19 pandemic," in *2021 2nd International Conference on Intelligent Engineering and Management (ICIEM)*, 2021, pp. 271–276.

[7] D. Kudathanthirige, D. Gunasinghe, and G. Amarasuriya, "Performance analysis of intelligent reflective surfaces for wireless communication," in *ICC 2020 - 2020 IEEE International Conference on Communications (ICC)*, 2020, pp. 1–6.

[8] Q. Wu, S. Zhang, B. Zheng, C. You, and R. Zhang, "Intelligent reflecting surface-aided wireless communications: A tutorial," *IEEE Transactions on Communications*, vol. 69, no. 5, pp. 3313–3351, 2021.

[9] X. Yuan, Y.-J. A. Zhang, Y. Shi, W. Yan, and H. Liu, "Reconfigurable-intelligent-surface empowered wireless communications: Challenges and opportunities," *IEEE Wireless Communications*, vol. 28, no. 2, pp. 136–143, 2021.

[10] Z. Chen, J. Tang, X. Y. Zhang, Q. Wu, Y. Wang, D. K. C. So, S. Jin, and K.-K. Wong, "Offset learning based channel estimation for intelligent reflecting surface-assisted indoor communication," *IEEE Journal of Selected Topics in Signal Processing*, vol. 16, no. 1, pp. 41–55, 2022.

[11] J. Sun, F. Khan, J. Li, M. D. Alshehri, R. Alturki, and M. Wedyan, "Mutual authentication scheme for the device-to-server communication in the internet of medical things," *IEEE Internet of Things Journal*, vol. 8, no. 21, pp. 15 663–15 671, 2021.

[12] Q. Chen, M. Li, X. Yang, R. Alturki, M. D. Alshehri, and F. Khan, "Impact of residual hardware impairment on the IoT secrecy performance of RIS-assisted NOMA networks," *IEEE Access*, vol. 9, pp. 42 583–42 592, 2021.

[13] Z. Hadzi-Velkov, S. Pejoski, N. Zlatanov, and H. Gaanin, "Designing wireless powered networks assisted by intelligent reflecting surfaces with mechanical tilt," *IEEE Communications Letters*, vol. 25, no. 10, pp. 3355–3359, 2021.

[14] X. Zhu, W. Zeng, and C. Xiao, "Precoder design for simultaneous wireless information and power transfer systems with finite-alphabet inputs," *IEEE Transactions on Vehicular Technology*, vol. 66, no. 10, pp. 9085–9097, 2017.

[15] J. Liu, K. Xiong, Y. Lu, D. W. K. Ng, Z. Zhong, and Z. Han, "Energy efficiency in secure IRS-aided SWIPT," *IEEE Wireless Communications Letters*, vol. 9, no. 11, pp. 1884–1888, 2020.